Review of Scientific Instruments

Kratky block-collimation small-angle x-ray diffractometer for synchrotron radiation

Cite as: Review of Scientific Instruments **58**, 1158 (1987); https://doi.org/10.1063/1.1139591
Submitted: 12 December 1986 . Accepted: 11 February 1987 . Published Online: 04 June 1998

Benjamin Chu, D.-Q. Wu, and C. Wu

View Online Export Citation

Lock-in Amplifiers up to 600 MHz Watch

AIP Publishing

© 1987 American Institute of Physics.

Kratky block-collimation small-angle x-ray diffractometer for synchrotron radiation

Benjamin Chu, D.-Q. Wu, and C. Wu

Chemistry Department, State University of New York at Stony Brook, Stony Brook, New York 11794-3400

(Received 12 December 1986; accepted for publication 11 February 1987)

A block slit collimation system of the Kratky design concept has been modified and adapted for synchrotron radiation. The building block small-angle x-ray diffractometer (SAXD) not only retains the essential advantages of the Kratky camera, i.e., accessibility at small values of $q[=(4\pi/\lambda)\sin(\theta/2)$ with λ and θ being the x-ray wavelength and the scattering angle, respectively] and ease of alignment, but also provides portability and low construction cost. With our SAXD operating at the SUNY X21A beamline of the National Synchrotron Light Source, we were able to reach $\theta \sim 1$ mrad corresponding to $q \sim 0.04$ nm^{-1} (or a Bragg spacing of 150 nm) using an incident slit width (d) of 0.5 mm and $\lambda = 0.15$ nm. At $d = 0.5$ mm, $\sim 10\%$ of the monochromatic synchrotron x-ray radiation passed through the block collimation system and a parasitic intensity to main beam intensity ratio of $\sim 10^{-5}$ at $\theta = 1$ mrad was achieved. With $d \sim 0.1$ mm, it is anticipated that $q \sim 0.01$ nm^{-1} can be accessible. By changing the vacuum tube length between the sample chamber and the beam stop from ~ 1400 to ~ 200 mm, we could reach an intermediate q range of $\sim 0.04 \lesssim q \lesssim 10$ nm^{-1} using a 5-cm-long linear position-sensitive detector with a resolution of $\sim 100\,\mu$m/channel. A description of the SAXD and its operation is presented.

INTRODUCTION

Small-angle x-ray scattering (SAXS) has been an established experimental discipline for many decades.[1,2] Although various collimation systems have been proposed to achieve experimental detection of x-ray small-angle scattering, the concept of a block-collimation system,[3,4] as first proposed by Kratky, has stood the test of time because of its simplicity in construction and ease of operation. An up-to-date summary of the Kratky camera with a more detailed description of a recently developed compact camera has been reported.[5]

The availability of synchrotron radiation together with recent advances in position-sensitive detectors (PSD)[6-10] has provided a renewed interest in small-angle x-ray scattering. Synchrotron radiation is tunable and very intense. The x-ray beam has a small ($\sim$0.1-mrad vertical $\times$5–10-mrad horizontal) divergence and a well-defined energy after monochromatization. By combining the desirable characteristics of the synchrotron x ray with PSD capabilities, time-resolved SAXS and anomalous SAXS become readily accessible and are powerful tools to study kinetics of material structural changes[11] in the SAXS range. The Kratky collimator has been used successfully for real-time studies of crazing processes in polymers at the Cornell High Energy Synchrotron Source[12] (CHESS). At intermediate q ranges in SAXS, primary beam collimation by pinhole diaphragms and/or slits has been more common.[13-15] After monochromatization and focusing the incident x-ray beam in the horizontal and vertical direction(s), the use of slits (mainly for line-shaped primary beams) or pinhole diaphragms (for primary beams with symmetrical circular cross sections) to eliminate parasitic radiation is applicable, provided that high resolution with q less than about a few tenths of nm^{-1} is not required. An alternative for accessibility to very low q values is the Bonse–Hart collimation system[16] which becomes more efficient than the Kratky block collimation system only for Bragg spacings greater than 700 nm.[2] Since our applications require an accessible q range of 0.01 nm$^{-1} \lesssim q \lesssim 10$ nm^{-1}, and in most cases isotropic samples, we have chosen the design concept of the Kratky block collimator. However, it should be noted that incident x-ray beams with square cross sections are available from the Kratky collimator leaving half of the scattering pattern free of parasitic radiation.[12] Thus, two-dimensional scattering patterns can be measured using the Kratky collimator.

I. MODIFICATION OF BLOCK COLLIMATION FOR SYNCHROTRON RADIATION

The SUNY small-angle x-ray diffractometer (SAXD)[15] without the Kratky block collimator has very limited q ranges. Based on the SUNY X21A beam optics, as listed in Table I, the incident x-ray beam at ~ 10 m from mirror H of Fig. 1, has very strong parasitic scattering in the vertical direction. Although the shape and cross section of the focused primary x-ray beam depend on the bent torroidal mirror, the use of a slit (or pinhole diaphragm) to alleviate the problem of small-angle scattering generated by the lead collimator G and mirror H (Fig. 1) based on the four-slit camera geometry designed by Beeman *et al.*[17,18] proved to be difficult to operate. Figure 2 shows a typical x-ray beam cross section at ~ 9.5 m (a), ~ 10 m (b), and ~ 11.5 m (c) from mirror H as shown in Fig. 1. At 9.5 m from mirror H, the incident x-ray beam shows very strong parasitic radiation in the vertical direction. It has an irregular shape because of focusing properties of the gold-coated bent torroidal quartz mirror as shown in Fig. 2(a). Generally, the beam

 0034-6748/87/071158-06$01.30 © 1987 American Institute of Physics

TABLE I. SUNY X21A beam optics.[15]

Source	X21 beam port at NSLS x-ray ring
Beamline	X21A 16-mrad branch line
Source size	$4\sigma_V \sim 0.4$ mm; $4\sigma_{V'}$ (incl. single electron emission angle) ~ 0.3 mrad; $4\sigma_H \sim 1.2$ mm; $4\sigma_{H'} \sim 0.8$ mrad
Type of optics	monochromator-focusing mirror optics
Monochromator	double-crystal fixed exit rapidly tunable monochromator with Si(111), Si(220), Ge(111) crystals available Bragg angle range 2°–45°
Mirror	bent torroidal quartz mirror (60 cm long, 6 cm radius), gold coated
Source–monochromator distance	7.4 m
Monochromator–mirror distance	1.5 m
Mirror–sample distance	~ 10 m
X-ray beam divergence	vertical 0.2 mrad, horizontal $\lesssim 7$ mrad
Expected x-ray intensity	Si(111)
Intensity[a] (photons/s)	$\sim 5 \times 10^{12}$
Energy resolution (eV)	4.8

[a] With loss factors of ~ 2.5 due to mirror, monochromator, He atoms, and windows already taken into account.

shape changes with distance, regardless of mirror orientation. After collimation by the modified Kratky block collimator, the well-defined primary x-ray beam has a cross section of $\sim 0.5 \times 3$ mm, as shown in Fig. 2(b). This is the beam cross section we use to design our sample chambers. Thus we insert an independent and separate collimator for SAXD.

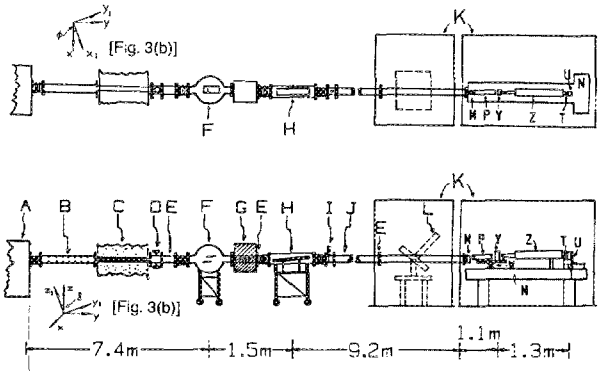

FIG. 1. Side view and top view of the SUNY beamline with the modified Kratky block collimator (B_1, B_2, and S as shown in Fig. 3). (A) front end, (B) acoustic delay line, (C) wall, wall piece, (D) tee piece, sensors, (E) Be windows, (F) monochromator, (G) lead collimator, (H) mirror, (I) photon shutter, (J) beam tubing, (K) hutches, (L) 4-θ goniometer, (M) ionization chamber, (N) optical bench (T-shaped, 1×9 ft^2 + 1×3 ft^2), (P) vacuum box with modified (B_1, B_2, S) Kratky block collimator, (T) beam stop, (U) linear position-sensitive detector, (W) jack for z adjustment, (Y) sample chamber, (Z) vacuum tube between Y and T.

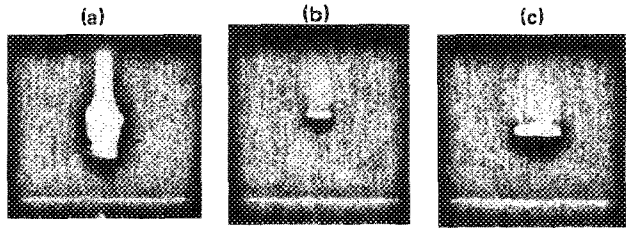

FIG. 2. (a) Typical incident x-ray beam cross section at ~ 9.5 m from mirror H, as shown in Fig. 1, revealing very strong parasitic radiation in the vertical (z) direction and an irregular shape because of focusing properties of the gold-coated bent torroidal quartz mirror. (b) Typical incident x-ray beam cross section at ~ 10 m from mirror H, after the modified Kratky collimator before the sample chamber Y as shown in Fig. 1. A line-shaped beam of ~ 0.5 mm width $\times$ a few mm length is observed. The beamwidth agrees with the variable slit (S) setting, i.e., $d \sim 0.5$ mm as shown in Fig. 3. The length of the primary beam can be partially controlled by the torroidal mirror H and by an external slit (defining aperture) as well as another horizontal slit (not shown; guard aperture) located between B_1 and B_2 blocks inside the vacuum box (P), as shown in Figs. 3 and 4. (c) Typical incident x-ray beam cross section at ~ 1.3 m from sample chamber Y. Location of primary x-ray beams in (b) and (c) are used to determine ψ, ϕ rotations while δ is adjusted according to magnitudes of parasitic radiation at small scattering angles. The primary beam intensity is optimized by a fine z adjustment (W) as shown in Fig. 4.

Our SAXD design also permits operation of SAXS at other synchrotron ports because of the block concept and integration of components on one optical bench.

Two special properties of synchrotron radiation, namely intrinsic collimation and larger beam cross sections, have been taken into account in modifying the Kratky block collimator. Figure 3(a) shows a schematic diagram of the modified Kratky block collimator for synchrotron radiation. The basic Kratky concept remains unchanged, i.e., no parasitic radiation is observed above the main section H (Fig. 3) defined by an exact coincidence of polished plane surfaces O_1 (top surface of block B_1) and O_2 (bottom surface of block B_2) in their mutual extension. Blocks B_1 and B_2 are separated by a distance $b = 402.0$ mm, mounted on an aluminum base ~ 13 mm thick, and prealigned with O_1 and O_2 surfaces in coincidence to within ~ 50 μm, the best which can be achieved by our machine shop. The condition for this crucial prealignment is relaxed because of an increase in b and a more directed synchrotron beam. A larger separation distance (b) is introduced so that we can accommodate the broader synchrotron beam. For example, if we take $b = 400$ mm and beamwidth in the vertical direction to be d, then $\delta \sim d/b = 2.5$ mrad for $d = 1$ mm. A block length of about half a meter is a compromise, since the size of the vacuum box, which demands δ, ϕ, ψ angular adjustments as shown in Figs. 1, 3(a), and 3(b), should not be too heavy. The vacuum box which holds the Kratky collimation system and has a ψ adjustment, the sample chamber, and the front end of the vacuum tube are mounted on an optical rail with ϕ and δ adjustments, as shown in Fig. 4. The optical rail is mounted on a precision jack with fine adjustments so that the primary x-ray beam intensity can be maximized. In the present configuration, slight movements of the synchrotron beam (σ of beam cross section) have little effect on the performance of our SAXD. Furthermore, alignment can be achieved easily even under less favorable operating conditions at a synchrotron beam port. We have opted for the building block system

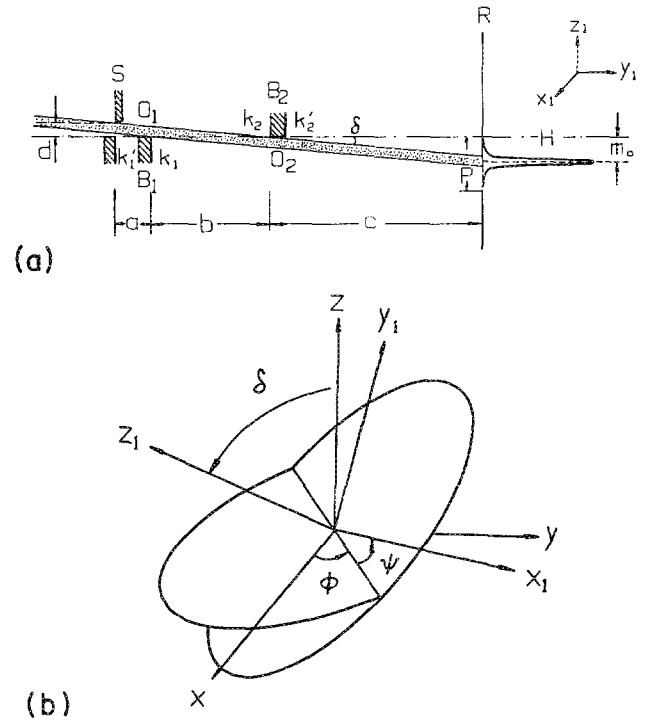

FIG. 3. (a) Section along the (y) direction of the synchrotron beam perpendicular to the (x, z) plane. Vertical (z_1) scale is multifold stretched compared to the horizontal y_1 axis. Variable entrance slit S and blocks B_1 (middle block) and B_2 (bridge) are perpendicular to the (x_1, z_1) plane. In the plane of registration R, the primary beam does not have a triangular (vertical) beam profile. A Gaussian-shaped intensity beam profile is presented schematically to emphasize that the synchrotron radiation (as denoted by the dotted area) is highly collimated. m_0 is the distance from the maximum intensity to the plane H. The Gaussian-shaped beam has fairly symmetrical long tails, mainly due to scattering by the edges k_1 and k_2. O_1 and O_2 represent the top surface of block B_1 and the bottom surface of block B_2, respectively. The SAXD dimensions are $a = 16.7$ mm, $b = 402.0$ mm, c = variable from ~ 0.2 to 1.5 m. Notations of Fig. 1 in Ref. 5, except for a,b,c,d, and δ, are preserved for a proper comparison. The subscript 1 denotes the coordinate system $(x_1y_1z_1)$ for the SAXD, where (xyz) denotes the coordinate system for the synchrotron primary beam after mirror H. We want $x \| x_1, z \| z_1$ and then tilt y_1 with angle δ between y and y_1 using x as the rotation axis. (b) Rotations defining Eulerian angles. ϕ is a coarse adjustment ($\sim 6\times 10^{-2}$ deg/division) which aligns synchrotron beam towards the y_1z_1 plane. ψ defines the horizontal (x_1, y_1) plane for the primary beam and has a micrometer adjustment with a sensitivity of 6×10^{-3} deg/division. ψ becomes more important for line-shaped primary beams. Variable slit S is prealigned to be parallel to the block surfaces O_1 and O_2. δ is the tilt adjustment for alignment of k_2S to the (y) direction of propagation of the primary synchrotron beam. The tilt adjustment has a sensitivity of $\sim 10^{-3}$ deg/division. δ changes with variable slit width d. All adjustments can be locked.

in order to accommodate variations in sample chamber requirements and in vacuum tube lengths before the detector. The increase in dimension in our modified Kratky block collimator has also made alignment less critical in absolute magnitudes of linear dimensions. With the use of ionization chambers and fluorescent screen/remote TV observation, our SAXD can be aligned much faster than a comparable Kratky building block camera using a conventional x-ray source.

II. INSTRUMENT CALIBRATION

We used a (variable) slit width (d) of ~ 0.5 mm to calibrate our SAXD. At $d \sim 0.5$ mm, the modified Kratky

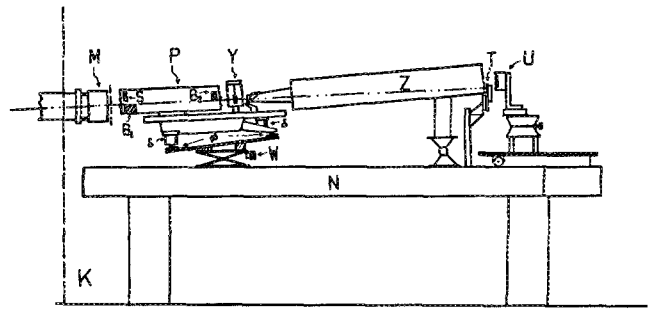

FIG. 4. Schematic diagram of SAXD with a modified Kratky block collimator. See Fig. 1 for notations: K,M,N,P,T,U,W,Y,Z; Fig. 3(a) for B_1,B_2,S. δ and ϕ denote rotational adjustments available to the optical bench on which P,Y and the front end of Z are located. ψ adjustment for the horizontal (x_1, y_1) plane is not shown.

collimator transmits $\sim 10\%$ of the incident x-ray intensity after monochromatization and beam focusing by the quartz torroidal mirror. For each slit width, we need to adjust the δ rotation and collimator height (h) so as to optimize the transmitted x-ray beam intensity and to minimize parasitic scattering. Figure 5 shows intensity profiles of the primary beam (inset) and ratios of parasitic scattering to main beam intensity (I/I_0) as a function of scattering angle [in terms of multichannel analyzer (MCA) channel number] after collimation by the modified Kratky block collimator at $c \sim 1.3$ m as shown in Fig. 2(c), measured in the vertical z direction.

At $\delta = 1.10$ mrad, which is comparable to the theoretical setting of $d/(a+b) = 0.5/(16.7+402.0) = 1.19$ mrad and $\theta \sim 1$ mrad, the primary beam profile shows a residual intensity corresponding to $\sim 4\times 10^{-4}$ of the total incident intensity. A magnitude of 10^{-4} in I/I_0 represents a greatly exaggerated estimate of parasitic scattering at $\theta \sim 1$ mrad because the LPSD tends to increase background counts in

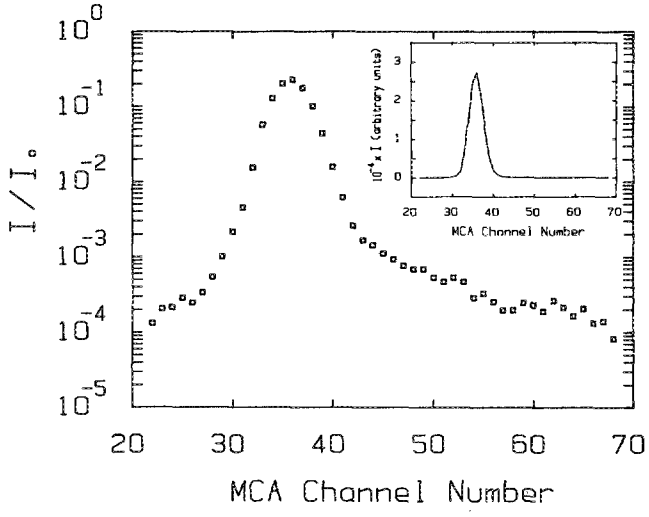

FIG. 5. Relative intensity profiles of the primary x-ray beam after collimation by the modified Kratky system [Fig. 3(a)]. Primary beam attenuated by a factor of $\sim 1.3\times 10^5$ using an aluminum block 0.90 mm thick. $d = 0.5$ mm, $c = 1.30\times 10^3$ mm. Braun LPSD has an angular resolution of (0.094 mm/c) $= 7\times 10^{-2}$ mrad and MCA channel number is in the positive z direction.

the presence of a high-intensity peak in neighboring positions. In Fig. 5 inset, the same primary beam is shown to have a peak position [m_0 of Fig. 3(a)] at channel number 36, and channels 30–42 contain 99% of the primary beam intensity. The minimum usable scattering angle θ_{min} (with a 0.5 mm beamwidth) is about 1 mrad, which corresponds to channel 50, equivalent to about 15 channels away from the peak intensity.

Figure 6 shows a plot of intensity ratio (%) versus relative collimator height (h) in mm. The intensity ratio denotes percent of primary x-ray beam intensity after and before the modified Kratky collimator as measured by the ionization chamber. The intensity profile qualitatively represents the original incident synchrotron beamwidth profile which has been smeared by the modified Kratky block collimator in the z direction [Fig. 3(b)]. Thus without the block collimator, the incident beamwidth is ~ 2 mm. Figure 6 also tells us that with $d = 0.5$ mm, small variations of incident synchrotron beam position of a few tenths mm will not change the throughput appreciably. At small scattering angles and for various (fixed) δ orientations, we could measure the amount of parasitic scattering as shown in Fig. 7.

In Fig. 7(a) we have plotted parasitic scattering intensity as a function of q (nm^{-1}) at three different fixed values of δ with $\delta = 1.10$ mrad (solid curve), 1.45 mrad (dotted curve), and 3.98 mrad (dashed curve) and $q = (4\pi/\lambda)\sin(\theta/2)$. The beam stop was set near $q \sim 0.06$ nm^{-1}. With $\delta = 1.10$–1.45 mrad, the amount of parasitic scattering at different scattering angles θ becomes essentially independent of the δ orientation as shown by the solid ($\delta = 1.10$ mrad) and dotted ($\delta = 1.45$ mrad) curves in Fig. 7(a). An intentional misalignment with $\delta = 3.98$ mrad shows an increase in parasitic scattering at small scattering angles ($q \lesssim 0.25$ nm^{-1}). Figure 7(b) shows plots of ratio of parasitic scattering to incident intensity (I/I_0) using two different beam-stop positions and $\delta = 1.10$ mrad. At $q = 0.044$ and 0.080 nm^{-1}, $I/I_0 \sim 7\times10^{-5}$ and 3×10^{-6}, respectively. Again, we note that once the block collimator has been aligned, the amount of parasitic scattering does not change

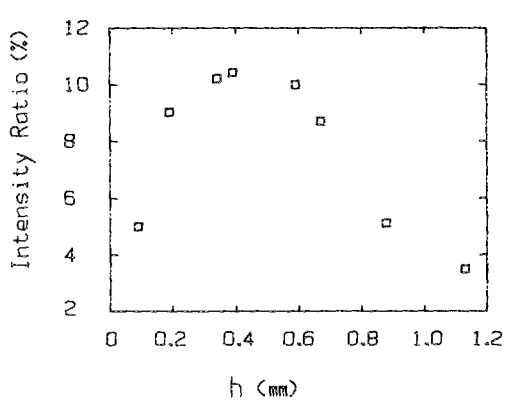

FIG. 6. Percent intensity ratio vs relative collimator height h (mm). Intensity ratio denotes % primary beam intensity after and before the modified Kratky collimator with $d = 0.5$ mm, as measured by two ionization chambers. This intensity profile qualitatively represents the synchrotron beamwidth profile at ~ 10 m after mirror H in the z direction [Fig. 3(b)].

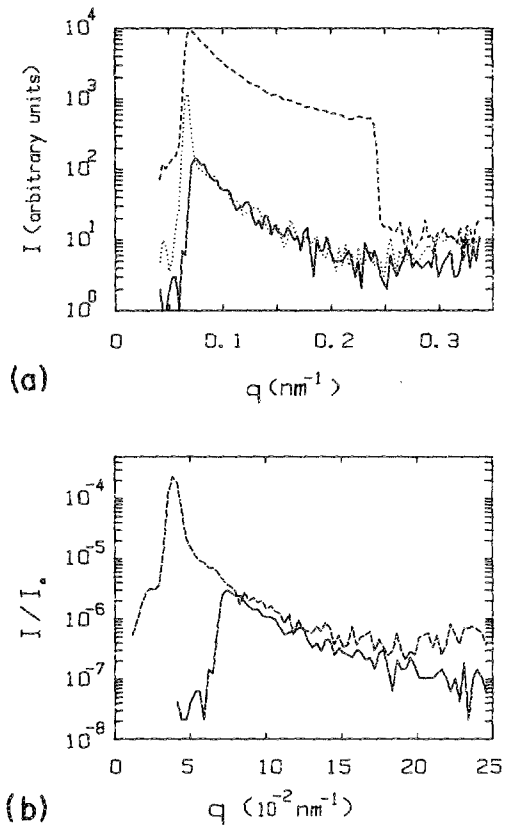

FIG. 7. (a) Parasitic scattering at fixed values of δ showing the importance of collimator block orientation in the δ direction. Solid line denotes $\delta = 1.10$ mrad; dotted line, $\delta = 1.45$ mrad; dashed line, $\delta = 3.98$ mrad. The low-intensity region ($q \lesssim 0.06$ nm^{-1}) represents the arbitrary beam-stop setting. The present estimates on parasitic scattering are more precise than those shown in Fig. 5 because the primary beam has been blocked by the beam stop. (b) Parasitic scattering at $\delta = 1.10$ mrad and two different values of beam-stop positions. Dashed line uses beam-stop position with $(I/I_0)_{max}$ at $q = 0.04$ nm^{-1}. Solid line uses beam-stop position with $I/I_0)_{max}$ at $q = 0.075$ nm^{-1}.

with the beam-stop positioning. From Fig. 7, it can be seen that the optimal setting is indeed close to $\delta \sim 1.19$ mrad, where a θ_{min} of ~ 1 mrad could be achieved, in agreement with the original design anticipation. With $\lambda = 0.15$ nm, $q = 0.04$ nm^{-1} corresponding to a Bragg spacing of 150 nm, where the intensity ratio of the main beam to parasitic scattering is $\sim 10^{+5}$. At $d \sim 0.5$ mm, our SAXD yields scattered intensities which are too intense for the Braun linear position-sensitive detector (LPSD), even for protein solutions. Thus for most cases, we should be able to reduce d, say to ~ 0.1 mm. At $d \sim 0.1$ mm, the increase in resolution of SAXD should be of the order of $q \sim 0.008$ nm^{-1} corresponding to a Bragg spacing of 750 nm. A Bragg spacing (D) of 750 nm is very respectable since with $\lambda_0 = 488$ nm from an argon-ion laser, $\theta = 90°$, and a refractive index of 1.5 for the scattering medium $D = 488/(3\times0.707) = 230$ nm in a typical light scattering measurement. One of our vacuum tubes (Z in Fig. 1 or c in Fig. 3) has a length of ~ 200 mm and the Braun LPSD has a linear range of 50 mm. With a resolution of ~ 0.5 mrad, our SAXD can cover 0.04 nm$^{-1} \lesssim q \lesssim 10$ nm^{-1} in one scattering-pattern measurement. The lower q range depends on the slit width d of the

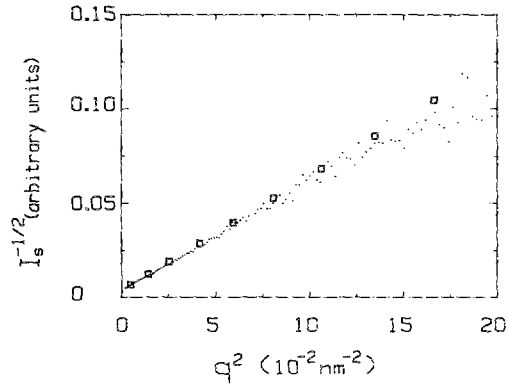

FIG. 8. Typical plot of $I_s^{-1/2}$ vs q^2 for a macroreticular resin sample Amberlyst 15. Dots represent relative scattered intensity after background and sample transmission corrections using synchrotron radiation but with incident intensity attenuated by a factor of ~400. Data were accumulated over a 100-s period. Hollow squares[19] denote relative scattered intensity after background, collimation, and sample transmission corrections using a standard Kratky camera x-ray source. $\xi = 12.8$ nm, in agreement with the literature value[19] of 13 nm.

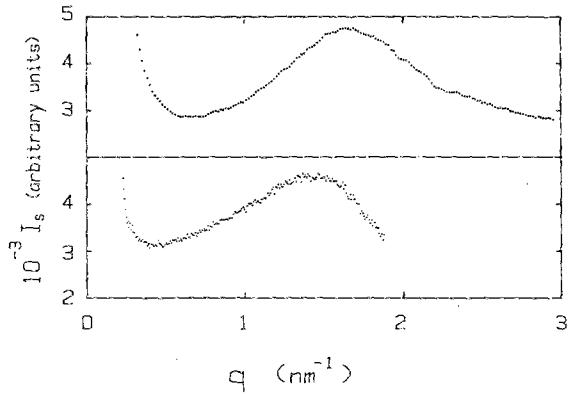

FIG. 9. Scattering patterns of a sodium salt of sulfonated polystyrene sample with 4.5 mol % S, $M_w = 1.15\times10^5$ g/mol, $M_w/M_n = 1.04$. Lower curve denotes the scattering curve after conventional background corrections using a slit source Kratky collimator, Cu$K\alpha$ radiation with generator settings at 40 kV and 25 mA, and a Braun LPSD. Exposure time was ~6 h.[22] No collimation corrections were made. Upper curve denotes the scattering curve of the same ionomer measured by our SAXD. The synchrotron radiation was attenuated ~130 times, c [as shown in Fig. 3(a)] = 250 mm. Exposure time was 1000 s. Only 1/2 of the scattering curve is shown for comparison purposes. No collimation corrections were needed for our scattering curve.

variable slit S as shown in Fig. 3(a). It should be noted that there have been many SAXD reported for the synchrotron radiation. The unique features of our SAXD are ease of alignment, portability, low cost, and covering a respectable q range ($0.04 \lesssim q \lesssim 10$ nm^{-1}) from one measurement of LPSD at a fixed vacuum tube length of ~200 mm and $q_{\min}$ ~0.008 nm^{-1} using a vacuum tube length of ~1500 mm and $d \lesssim 0.1$ mm. Thus our SAXD are appropriate for most supramolecular systems, including polymer solutions, melts, and solids, as well as colloidal suspensions. With the addition of a two-dimensional detector, it is also suitable for SAXS of anisotropic systems.

III. EXPERIMENTAL DEMONSTRATIONS

Small-angle x-ray scattering from a macroreticular sulfonic acid cation-exchange resin-Amberlyst 15[19] shows a correlation length $\xi = 13$ nm where, for a random distribution of inhomogeneities in the electron density, the correlation function $C(r) = \exp(-r/\xi)$ and the scattered intensity has the form $I_s^{-1} \sim (1 + \xi^2 q^2)^2$. In a plot of $I_s^{-1/2}$ vs q^2 as shown in Fig. 8, we get $\xi = 12.8$ nm, in agreement with the literature value of 13 nm.

There has been some dispute in the interpretation of SAXS data by ionomers using interparticle[20] or intraparticle[21] interference models. Better scattering patterns, together with other analytical techniques, such as extended x-ray absorption fine structure (EXAFS), may lead toward a better understanding of the microstructure of ionomers. Figure 9 shows typical scattering patterns of a sodium salt of sulfonated polystyrene sample (4.5 mol % S, $M_w = 1.15\times10^5$ g/mol, $M_w/M_n = 1.04$). By conventional means, the lower scattering curve took about 6 h.[22] By using our SAXD, the scattering pattern could be obtained in minutes, demonstrating the enormous usable throughput of our SAXD. A position-sensitive detector with a much higher dynamic range than the Braun LPSD is needed for time-resolved studies.

ACKNOWLEDGMENTS

We gratefully acknowledge support of this work, including design and construction of the SAXD, by the Department of Energy (DEFG0286ER45237A000) and the U. S. Army Research Office. BC wishes to thank J. Phillips and A. LeGrand for their assistance in using the SUNY X21A2 beam line, supported by the Department of Energy (DEFG0286ER45321A001) at the National Synchrotron Light Source, Brookhaven National Laboratory, Upton, New York.

[1] A. Guinier and G. Fournet, *Small Angle Scattering of X-rays* (Wiley, New York, Chapman and Hall, London, 1955).
[2] *Small Angle X-ray Scattering*, edited by O. Glatter and O. Kratky (Academic, London, 1982).
[3] O. Kratky, Z. Elektrochem. **58**, 49 (1954); **62**, 66 (1958).
[4] O. Kratky and Z. Skala, Z. Electrochem. **62**, 73 (1958).
[5] O. Kratky and H. Stabinger, Colloid. Polym. Sci. **262**, 345 (1984).
[6] A. Gabriel, Rev. Sci. Instrum. **48**, 1303 (1977).
[7] A. R. Faruqi and C. C. Bond, Nucl. Instrum. Methods **201**, 125 (1982).
[8] A. R. Faruqi, IEEE Trans. Nucl. Sci. **NS-30**, 358 (1983).
[9] W. Prieske, C. Rickel, M. H. J. Kock, and H. G. Zachmann, Nucl. Instrum. Methods **208**, 435 (1983).
[10] M. Caffrey and D. H. Bilderback, Nucl. Instrum. Methods **208**, 495 (1983).
[11] T. P. Russell and A. N. Goland, Polym. Res. at Synchrotron Radiation Sources, BNL 51847, UC-25 (Materials-TIC-4500), National Technical Information Service, U.S. Department of Commerce, Springfield, VA, 1985.
[12] H. R. Brown, P. J. Mills, and E. J. Kramer, Ref. 11, pp. 29–35.
[13] J. Hendrix, M. H. J. Koch, and J. Bordas, J. Appl. Crystallogr. **12**, 467 (1979).
[14] Y. Amemiya, K. Wakabayashi, T. Hamanaka, T. Wakabayashi, T. Matsushita, and H. Hashizume, Nucl. Instrum. Methods **208**, 471 (1985).
[15] B. Chu, J. Phillips, and D.-Q. Wu, Ref. 11, pp. 126–132.
[16] U. Bonse and M. Hart, in *Small Angle X-ray Scattering*, edited by H.

Brumberger (Gordon and Breach, New York, 1967).
[17]H. N. Ritland, P. Kaesberg, and W. W. Beeman, J. Appl. Phys. **21**, 838 (1950).
[18]J. W. Anderegg, W. W. Beeman, S. Shulman, and P. J. Kaesberg, J. Am. Chem. Soc. **77**, 2927 (1955).
[19]B. Chu and D. M. Tan Creti, J. Phys. Chem. **71**, 1943 (1967).
[20]D. J. Yarusso and S. L. Cooper, Macromolecules **16**, 187 (1983).
[21]W. J. MacKnight, W. P. Taggart, and R. S. Stein, J. Polym. Sci. Polym. Symp. **45**, 113 (1974).
[22]W. J. MacKnight (private communications).